Role of tip apices in scanning force spectroscopy on alkali halides at room temperature—chemical nature of the tip apex and atomic-scale deformations

OPEN ACCESS
IOP Publishing
Nanotechnology

Nanotechnology **32** (2021) 035706 (10pp)
https://doi.org/10.1088/1361-6528/abbea8

Role of tip apices in scanning force spectroscopy on alkali halides at room temperature—chemical nature of the tip apex and atomic-scale deformations

Philipp Wagner[1], Adam Foster[2,3,4], Insook Yi[5], Masayuki Abe[5], Yoshiaki Sugimoto[5] and Regina Hoffmann-Vogel[6,7]

[1] Physikalisches Institut, Karlsruher Institut für Technologie, D-76128 Karlsruhe, Germany
[2] Department of Applied Physics, Aalto University School of Science, PO Box 11100, FI-00076 Aalto, Finland
[3] WPI Nano Life Science Institute (WPI-NanoLSI), Kanazawa University, Kakuma-machi, Kanazawa 920-1192, Japan
[4] Graduate School Materials Science in Mainz, Staudinger Weg 9, D-55128, Germany
[5] Graduate School of Engineering, Osaka University, Japan
[6] Department of Physics, University of Konstanz, Universitätsstrasse 10, D-78464 Konstanz, Germany
[7] Institute of Physics and Astronomy, University of Potsdam, Karl-Liebknecht Strasse 24-25, D-14476 Potsdam-Golm, Germany

E-mail: regina.hoffmann-vogel@uni-potsdam.de

Received 17 June 2020, revised 7 September 2020
Accepted for publication 6 October 2020
Published 22 October 2020

Abstract

We have revealed processes of the tip apex distortion in the measurements of non-contact scanning force microscopy. High-spatial-resolution two-dimensional force mapping on KCl (100) surfaces for a large number of tips, seven tips, enabled us to see the complex behavior of the tip apex distortion. The tips are from Si without additional coating, but are altered by the tip-sample interaction and show the behavior of different atomic species. On the KCl(001) surfaces, the tip apex, consisting of K and Cl atoms or of Si, distorted several times while changing the distance even in a weak attractive region. There are variations in rigidity of the tip apex, but all tips distorted in the small attractive region. This complex behavior was categorized in patterns by our analyses. We compare the experimental force–distance data to atomistic simulations using rigid KCl-terminated tips and KCl-terminated tips with an additional KCl-pair designed to perform atomic jumps. We also compare the experimental force–distance data to first principles simulations using Si tips. We mainly find K-terminated tips and Si-terminated tips. We find that Si tips show only one force minimum whereas KCl-terminated tips show two force minima in line with the stronger rigidity of Si compared to KCl. At room temperature, the tip apex atoms can perform atomic jumps that change the atomic configuration of the tip apex.

Keywords: scanning force microscopy, insulating surfaces, tip-sample interaction

(Some figures may appear in colour only in the online journal)

1. Introduction

Non-contact scanning force microscopy (NC-SFM) also called non-contact atomic force microscopy has become a

valuable tool for investigating not only insulating surfaces, but also for determining tip-sample interactions at the atomic scale [1–3]. It allows to bring a tip within a distance of fractions of an atom to an atomic site on the surface and study its interaction with the surface with utmost precision. In addition, scanning force microscopy has allowed to know the charge of the tip-apex atom and to identify the chemical nature of surface atoms [4–6] even on alkali halide surfaces where they only differ by their charge [7, 8]. Alkali halide surfaces have been particularly important during the development of NC-SFM. Recently, they have served as insulating substrates for molecules [9–12] and for intercalation of graphene layers [13] studied by NC-SFM. Often in these studies it cannot be avoided that the tip is covered by sample material through the interaction with the sample.

At close tip-sample distances, the tip strongly interacts with the surface through interatomic interactions. These interactions strongly deform the tip-apex. Such deformations have been studied before, mainly to explain atomic-scale energy dissipation [14, 15]. For NaCl surfaces, it has been found that atomic chains can be drawn from the surface [16, 17]. For KBr, it has been concluded that the tip is soft [18]. The chemical nature of the tip—whether it is covered by sample material and what ion terminates its apex as well as the atomic motion of the frontmost atoms interacting with the sample has a strong impact on NC-SFM image formation.

Here, we investigate the tip-sample interaction on the KCl surface. We show atomic-scale tip-sample interaction curves as a function of distance for a large number of tips, i.e. seven tips. The force–distance results of the tips individually differ although Si tips without additional coatings are used in all cases. The atomic state of the tip apex differs for each tip after the interaction with the KCl surface. We can find several categories of tips. For one group, showing only one force minimum, the tip is best described by a rigid neutral Si tip. Calculations show that Si tips show only small elastic deformations and atomic deformations and atomic tip-sample interactions can explain the shape of the overall force–distance data that is observed experimentally. For another group, showing two force minima, the tip is best described by loosely bound KCl ions attached to the tip. The deformation from these loosely bound ions strongly deform the force–distance data. Since we do not observe stable KCl tips, we conclude that KCl only loosely attaches to the Si tip.

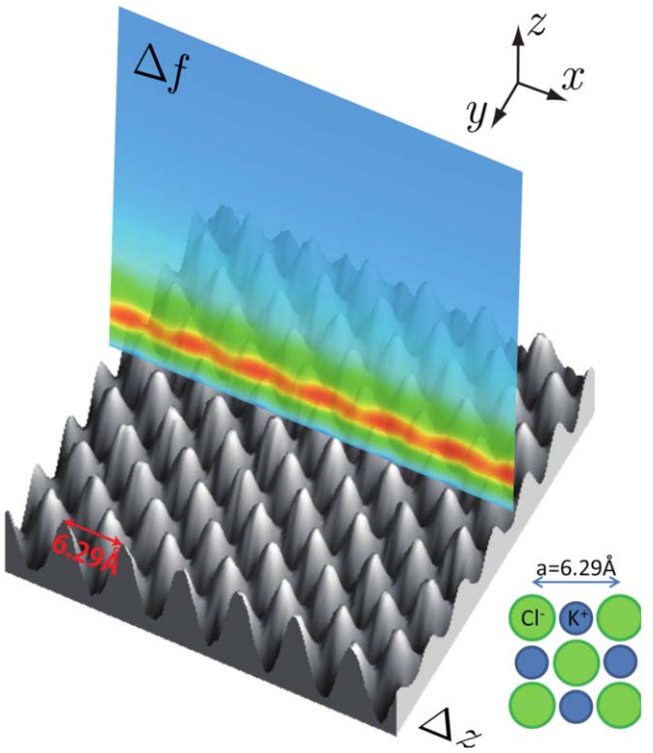

Figure 1. Bird's-eye view of NC-SFM topographic image (Δz, gray, non-filtered) and two-dimensional frequency shift map (Δf, color) on a KCl(001) surface. Thermal drift compensation was activated during the acquisition of both data. The Δf mapping was performed along [100] direction (x direction). In Δf mapping, 1024 × 1024 points were measured for 3.4 min. Resonance frequency, spring constant, and oscillation amplitude of cantilever were $f_0 = 163$ kHz, $k = 30.2$ N m^{-1}, and $A = 75$ Å, respectively, and the set point value for topography imaging was $\Delta f = -20.7$ Hz.

2. Experimental methods

The experiments were performed in a home-build ultra-high vacuum chamber equipped with a scanning force microscope mostly similar to the one described in detail in [19]. Cleaving KCl single crystals (Furuchi Chemical, purity 99.9%) in air resulted in atomically flat KCl(001) surfaces. The samples were transferred to the vacuum chamber immediately after cleavage. Subsequently the chamber was baked-out at about 100 °C for 12 h. Silicon cantilevers (Nanoworld, Neuchatel, Switzerland) with standard tips and spring constants of about 30 N m^{-1} and resonant frequencies of about 160 kHz were cleaned by Ar ion sputtering in ultrahigh vacuum to remove the natural oxide layer at the tip apex. For imaging at room temperature we used dynamic NC-SFM with frequency shift detection [20]. The tip-sample distance during imaging was controlled by keeping the frequency shift constant. The electrostatic interaction arising from the contact potential difference between tip and sample was minimized by applying a constant voltage between tip and sample. For force–distance measurements, the control of the frequency shift was switched off, the tip was retracted from the surface and subsequently approached while slowly varying the lateral position (x-direction) as described in detail in [21]. Data slices, see figure 1, mostly oriented along the [100]-direction were acquired. In one data slice the [110]-direction was used. During imaging as well as during frequency shift versus distance measurements, thermal drift compensation was activated using the atom-tracking technique. The accuracy of the drift compensation depends on the tip condition and on the Δf noise. It is ±0.1 Å typically. Overview images of the surface show steps mostly oriented along the [100] direction. In addition, some wedge-shaped cleavage steps remained on the surface. Residual charge decorated the steps. More details about the experiment can be found in [22].

3. Experimental results and discussion

After acquiring such overview images, we reduced the image size and continued to approach the tip to the surface to obtain atomic resolution images. Figure 1 describes an overview of the sample surface and the measurement configuration: the sample has NaCl configuration and a lattice constant of $a = 6.29$ Å [23]. During imaging the characteristic pattern of positively and negatively charged ions is found that is typical for NaCl-type surfaces. Each topographic maximum corresponds to one type of atom and each topographic minimum corresponds to the other type of atom. Then force distance measurements were started. In addition, an example of a two-dimensional slice of measured frequency shift versus distance data is overlaid. The slice is taken along the [100] direction of the surface and shows atomic resolution.

Figure 2 shows a comparison of the measured frequency shift data for all of the different tips used together with force maps obtained from conversion of the frequency shift to force using Sader's method [24]. The data obtained near the surface has been cut from data measured between 0 and 2–3 nm distance from the surface. All measurements show atomic resolution. In many cases there are more than one maximum of attractive force observed as a function of tip-sample distance.

Figure 3 shows again the data obtained for tip 1 (see figures 2(a) and (b)). From the data, frequency shift and force versus distance data obtained above a topographic maximum are shown as an example. Not only in the force as a function of distance, but also in the frequency shift, one can observe that there are several maxima as a function of distance. This also becomes clear from the line profiles showing the frequency shift in figure 3(d): with increasing tip-sample distance, the amplitude of the oscillation caused by atomic resolution generally decreases. However, for line profile number (4) the amplitude *increases* with respect to the line profile obtained at closer tip-sample distances, number (5). The green dashed line serves as a guide to the eye and helps to compare the lateral (x-) position of the maxima and minima corresponding to the position of atoms: whereas the dashed green line marks a maxima in curve (10), it marks a minimum in curve (7) and again a maximum in curve (4). In addition, some line profiles show split peaks, such as the line profiles number (9), (8) and (5).

It should be carefully excluded that the oscillations of tip-sample force as a function of distance could be caused by the ill-posedness of the inversion problem [25]. Figures 3(c) and 4(c) show that the original frequency shift data does not show inversion points which are responsible for the ill-posedness. Instead, we attribute these oscillations of the tip-sample force to atomic relaxations.

It has been proposed that, due to bending of the tip, the lateral position of the measurement could vary as a function of tip-sample distance [26]. A postprocessing correction has been applied to minimize the effect of drift and creep, but such a procedure can never fully compensate all deformations and often leads to artefacts. We stress that here drift compensation was activated during data acquisition. As a consequence we expect residual thermal drift effects to be small. It is remarkable that oscillations in the force as a function of tip-sample distance remain even for tips where the measured data is symmetric with respect to the crystallographic directions of KBr. At least for these cases, the oscillations cannot be explained by an overall bending of the more mesoscopic tip. To better understand the origin of the observed phenomena, we model the tip deformations at the atomic scale.

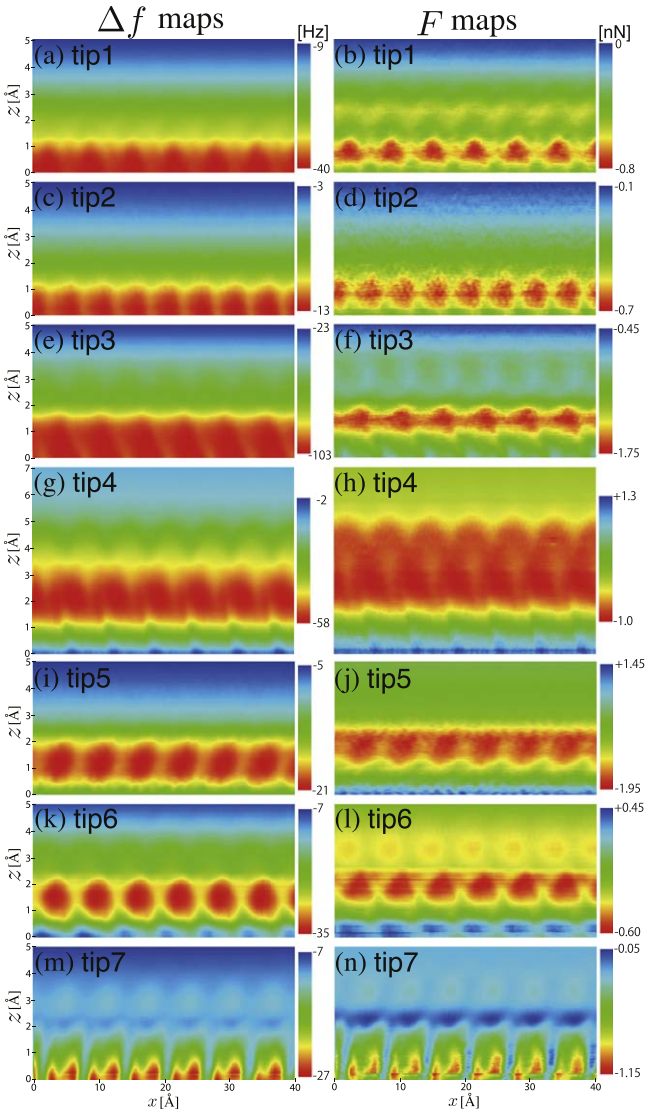

Figure 2. Frequency shift (Δf, left column) and inverted force (F, right column) maps on the KCl surface acquired at room temperature. The lateral axes is the direction along the sample surface, the vertical axes is the distance between tip and sample. The color scale encodes the measured frequency shift (left column) and the force (right column) obtained by numerical conversion from the measured frequency shift data. The conversion inverts the integral taken on the force over the distance of the oscillation during one oscillation cycle and changes the shape of the data. Different SFM tips were used for the map acquisitions. Here, maps close to the surface ($z = 5$ or 7 Å, $x = 40$ Å) were trimmed from the original ones. Note that each map has a different color scale range.

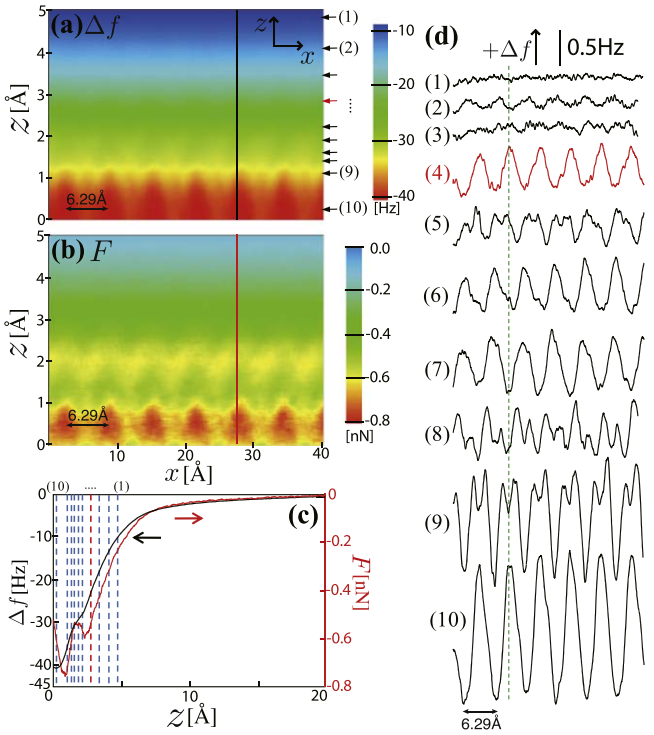

Figure 3. Results and analyses of two-dimensional force mapping performed on a KCl(001) surface. The data is the same as the map of figures 2(a) and (b) using tip 1. (a) Two-dimensional Δf map acquired on the KCl(001) surface, and (b) total force F map inverted from (a). As in figure 2 only the distance region close to the surface ($z = 5$ Å, $x = 40$ Å) is shown. The oscillation amplitude, spring constant, and resonance frequency of the cantilever for both imaging and mapping were $A = 83$ Å, $k = 32.0$ N m^{-1}, and $f_0 = 166$ kHz, respectively. (c) Distance-dependent data obtained from $\Delta f(z)$ (black curve) and $F(z)$ (red curve) maps, which corresponds to the data shown at the position of the black line in (a) and that at the red line in (b), respectively. (d) Line profiles of Δf map at the points of arrows (1)–(10) of (a). Numbers of (1)–(10) correspond to distance of $z = 4.8$, 4.1, 3.4, 2.8, 2.2, 1.9, 1.6, 1.4, 1.1, and 0.2 Å, respectively. Corresponding distances of (1)–(10) are also shown with dashed lines in (c).

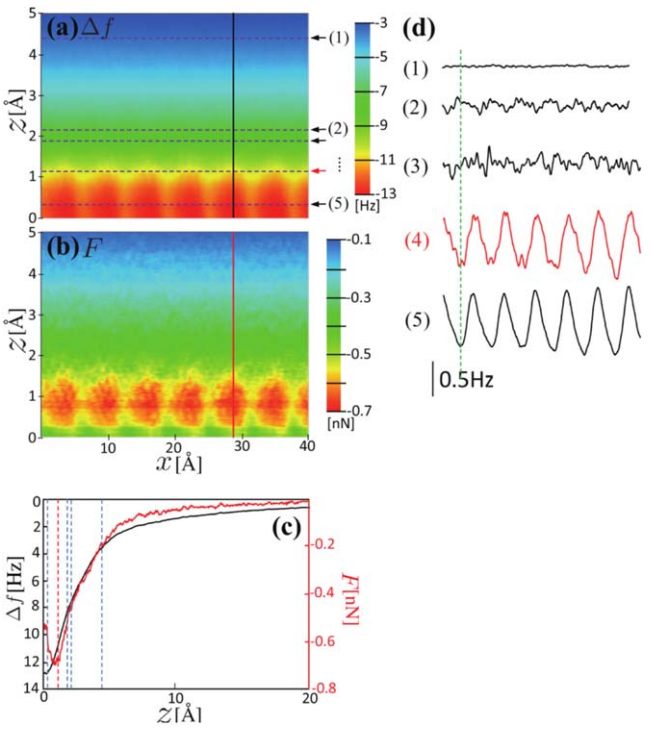

Figure 4. Results and analyses of two-dimensional force mapping performed on a KCl(001) surface with a tip 2. (a) Two-dimensional Δf map acquired on a KCl(001) surface, and (b) total force F map inverted from (a). The oscillation amplitude, spring constant, and resonance frequency of the cantilever for both imaging and mapping were $A = 180$ Å, $k = 29.5$ N m^{-1}, and $f_0 = 168$ kHz, respectively. (b) $\Delta F(z)$ (black) and inverted $F(z)$ curve (red) on the KCl(001) surface. The $\Delta F(z)$ is the line profile along the black vertical dashed line in part (a). (c) Line profiles of (a) (black) and (b) (red) along the black and the red lines, which corresponds to $\Delta f(z)$ and $F(z)$ curves, respectively. (d) $\Delta f(x)$ curves along dashed lines (1)–(5) in (a) and (c). Distances of (1)–(5) are $z = 4.4$, 2.1, 1.8, 1.1, and 0.3 Å, respectively.

4. Computational methods

The calculations were performed following a procedure described previously [7, 15]. The ionic interaction forces were computed using pairwise Buckingham potentials. In addition the polarizability of the ions was represented using a core–shell model. The parameters were taken from [27]. The sample was represented by 600 KCl ions. Two different sets of calculations were performed with two different models for the tip. The first tip was modeled using a cluster of $4 \times 4 \times 4$ KCl ions oriented such that one corner of the cube was facing the sample surface. For the second tip model, one additional K and one additional Cl ion were added to the tip apex. The tip was put in the vicinity of the sample with its apex above a pre-chosen site above the KCl unit cell. It was then gradually approached to the sample surface. At each tip-sample distance, tip and sample atoms were moved numerically until equilibrium was obtained, i.e. the atoms were allowed to undergo relaxation of their atomic positions. The topmost part of the tip and the bottom layer of the sample were kept fixed during the relaxation.

In addition, first principles calculations were performed using Si tips. In these calculations we used the periodic plane-wave basis VASP code [28, 29] implementing the spin-polarized density functional theory. To accurately include van der Waals interactions in this system we used the optB86B +vdW-DF functional [30–32]. Projected augmented wave potentials were used to describe the core electrons [33], with a kinetic energy cutoff of 550 eV (with the precision parameter 'prec' set to the value 'accurate'. - `PREC = accurate`). Systematic k-point convergence was checked for all systems, with sampling chosen according to system size and a mesh of $5 \times 5 \times 1$ being used for the final production runs. This approach converged the total energy of all the systems to the order of meV. The properties of the bulk and surface of KCl were carefully checked within this methodology, and excellent agreement was achieved with experiments. For calculations of the tip-surface system, a surface slab of $6 \times 6 \times 4$ in terms of the KCl unit cell was used, along with a dimer cluster tip [34] with a vacuum gap of at least 1.5 nm. The upper three

layers of KCl and bottom three layers in the tip are allowed to relax.

5. Comparison of experimental and theoretical data

5.1. Separation of long-range and short-range forces

To compare the experimental force–distance data with the calculated ones, we mainly focus on the data obtained at the position where the two atomic species are located. The lateral (x-) positions of the atoms are spaced by half a KCl lattice constant, ideally 0.3147 nm [23, 27]. Due to calibration errors or thermal drift the actual spacing of the atoms could slightly deviate from this distance. First, the lateral position of the ions charged oppositely to the tip apex atom (strongest attraction) was determined mathematically as the lateral position of a local minimum in the force in the x and in the tip-sample distance (z-direction). To find the lateral positions of the equally charged ions, the slice was filtered and mathematically cut into pieces of half a lattice constant length around the positions of the oppositely charged ions. Then the point of minimum force in z-direction and maximum force in x-direction was determined for each slice. The results are shown for one example (tip 4) in figure 5(a). The force–distance data obtained at these positions was averaged over all atoms of the same type.

We then determined the long-range forces from the total measured force. Since only the short-range forces depend on the atomic position, the long-range forces were determined from the average of all 1024 curves of the slice. Only distances larger than the point $z_1 = 0.6$ nm, where the forces on the different atomic sites differed, were used for fitting. We considered the van-der-Waals force for a cone with a spherical cap [35, 36]

$$F_{\mathrm{vdW}} = -\frac{C_{\mathrm{H}}}{6}\left(\frac{R}{z^2} + \frac{\tan^2(\alpha)}{z + R_\alpha} - \frac{R_\alpha}{z(z + R_\alpha)}\right), \qquad (1)$$

where the tip radius is R, the opening angle of the cone is α, R_α denotes $R(1 - \sin(\alpha))$ and C_{H} is the Hamaker constant of the material. If an additional electrostatic force F_{elec} were relevant the total long-range forces would be $F_{\mathrm{tot}} = F_{\mathrm{vdW}} + F_{\mathrm{elec}}$. However, we found the long-range forces were well-described by a van-der-Waals force and an electrostatic contribution was not needed. We are confident that there is no significant electrostatic force included in the measured force data, because it would cause the fitted tip radius of the van-der-Waals model to increase. The tip opening angle was chosen to be 10° according to the value given by the manufacturer and the Hamaker constant $C_{\mathrm{H}} = 0.371$ eV [37]. By manual adjustment, we obtained tip radii between 1.2 and 4.3 nm, see table 1. The tips have an average radius of 3.4 nm with a standard deviation of 0.75 nm. These values are in good agreement with the information given by the manufacturer, stating that the tip radius is below 8 nm. These small fitted tip radii obtained from the van-der-Waals model fit confirm that the electrostatic force is small.

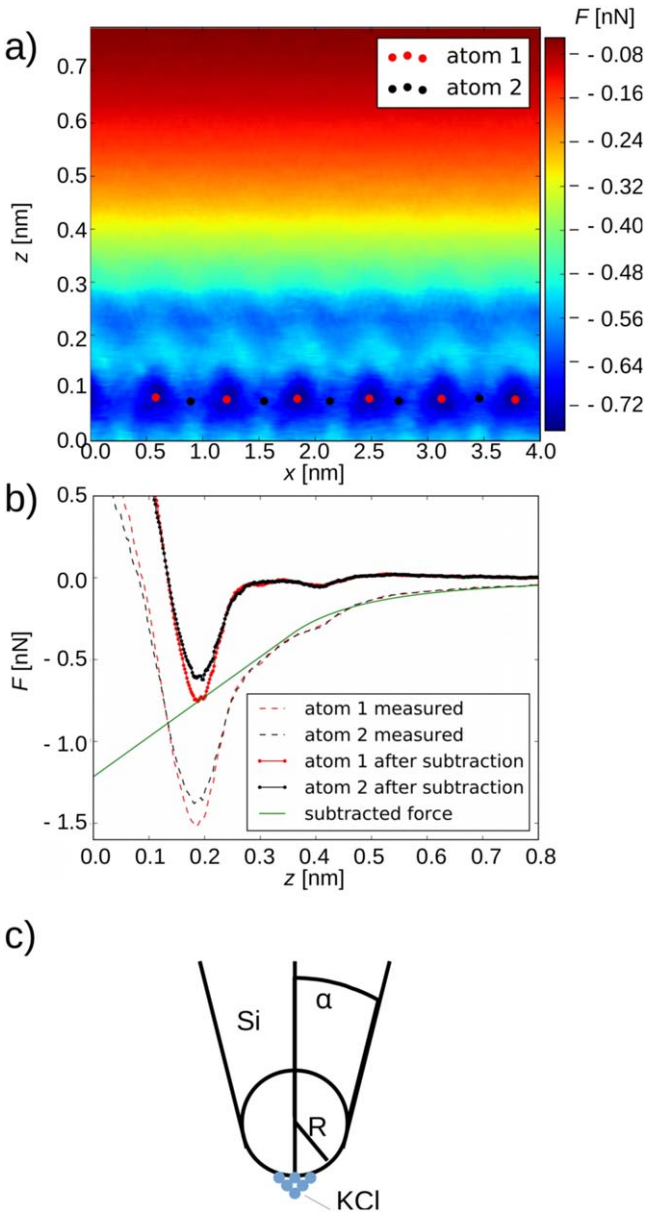

Figure 5. (a) Example of lateral atomic positions used for averaging. (b) Averaged experimental data measured over the two major atomic positions using tip 4 in dashed red and black lines. The description of the long-range force is also given in green. The short-range forces obtained after subtraction are shown in drawn out red and black curves. (c) Model of the tip used for the calculation of the long-range forces.

Table 1. Tip apex radii obtained from fitting the van-der-Waals forces to the force–distance data as described in the text. Tip seven was excluded from the analysis because it shows a double tip. For tip eight only data along the [110] direction was obtained.

Tip number	1	2	3	4	5	6
Fitted tip apex radius (nm)	3.5	4.2	4.3	3.5	1.2	4.3

For small tip-sample distances z the mathematically given van-der-Waals force diverges. However, since the formula is based on continuous medium without atomic composition this could be unrealistic at these distances. In the

region below $z_1 = 0.6$ nm, equation (1) is no longer a good approximation. Instead, we use a method introduced in [8]: at the point where the fitted van-der-Waals force and the measured force–distance curve begin to separate, the long-range force is approximated by a straight line. This is reasonable because in a small range of z the forces increase proportionally with distance. This behavior corresponds to Hook's law and could be caused by an elastic relaxation of tip and/or sample. Due to the short tip-sample distances where it occurs and due to the geometry of the problem, it is likely that this elastic deformation occurs between a few atoms of the tip apex.

The result of subtracting the long-range forces determined in this way is shown in figure 5(b). After subtraction of the long-range forces, most of the force–distance data can be categorized into two groups, one showing one force minimum as a function of z and the other showing two force minima. Only one tip cannot be grouped in these two categories due to the weak tip-sample interaction. In the following, we compare experimental data with calculated results for all three types of force curves.

5.2. One force minimum—Si tip

Three tips with data sliced along the [001] direction showed one force minimum with a maximal attractive force above 0.5 nN, tips No. 3 and 4 and an additional data set described below. An example for the force–distance data is shown in figure 6 which shows tip 3. When comparing the force–distance data with the calculations, the force–distance data for the oppositely charged ions in both figure 6(a) showing the K-terminated tip and (b) showing the Cl-terminated tip are well-described in both cases. At the same time the force–distance data for the similarly charged ions strongly differ from the calculated ones, also for both tip terminations. Such a behavior had been found previously in NaCl [38]. For NaCl, a large number of different tips were investigated in simulations but none could explain the observed behavior. The conclusion was drawn that these experimental observations could be explained in the best way by a neutral Si tip.

An additional data set sliced along the [110] direction fits into this interpretation, see figure 7. The measured slice along the [110] includes a measurement on top of one type of atom, the oppositely charged one, and the center of the unit cell located between two equally and two oppositely charged ions. Along this direction, experimentally two minima of nearly the same amplitude and nearly the same distance to the surface are found on the maximum attractive site and on the center of the unit cell. The calculations suggest that the K-terminated tip should show two force minima of nearly the same amplitude and nearly the same distance to the surface, on the maximum attractive site and the center position of the unit cell. For the Cl-terminated tip, one obtains two force minima of nearly the same amplitude at different distances to the surface.

Neither of the calculated tips represent the experiment well. In the simulations, the force minimum above the center of the unit cell occurs in all cases at positions closer to the surface compared to the force minimum calculated above the attractive ion. This occurs because lateral forces from the neighboring surface sites counterbalance each other due to the symmetric charge distribution above the center of the unit cell. In the experiment, this is not observed. This is a sign that the counterbalancing of forces caused by positively and negatively charged ions plays a minor role here, and that other forces dominate the tip-sample interaction as we expect for a neutral Si tip.

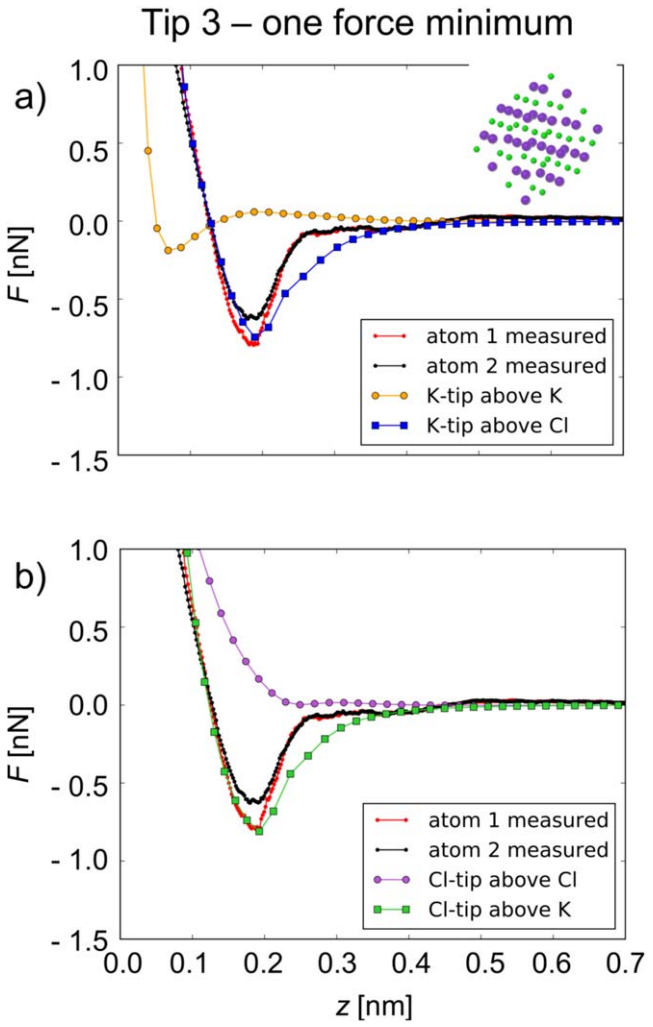

Figure 6. (a) Comparison of force–distance data obtained using tip 3 showing only one force minimum with the calculated results using a K-terminated tip. (b) Comparison with the calculations using a Cl-terminated tip.

In an effort to make this comparison more rigorous, we performed further calculations for Si tips using a first principles approach as described in the section on computational methods. The results of these simulations are shown in figure 8. We observe an initially stronger interaction with K until close approach where the interaction with Cl dominates. At around 0.3 nm we also observe a jump of a Cl ion to the tip and a resultant very large increase in the attractive force. Even ignoring this, we observe that while the magnitude of the force agrees with experiment (maximum around 0.5 nN), as do the difference in magnitudes (about 0.1 nN), the maxima

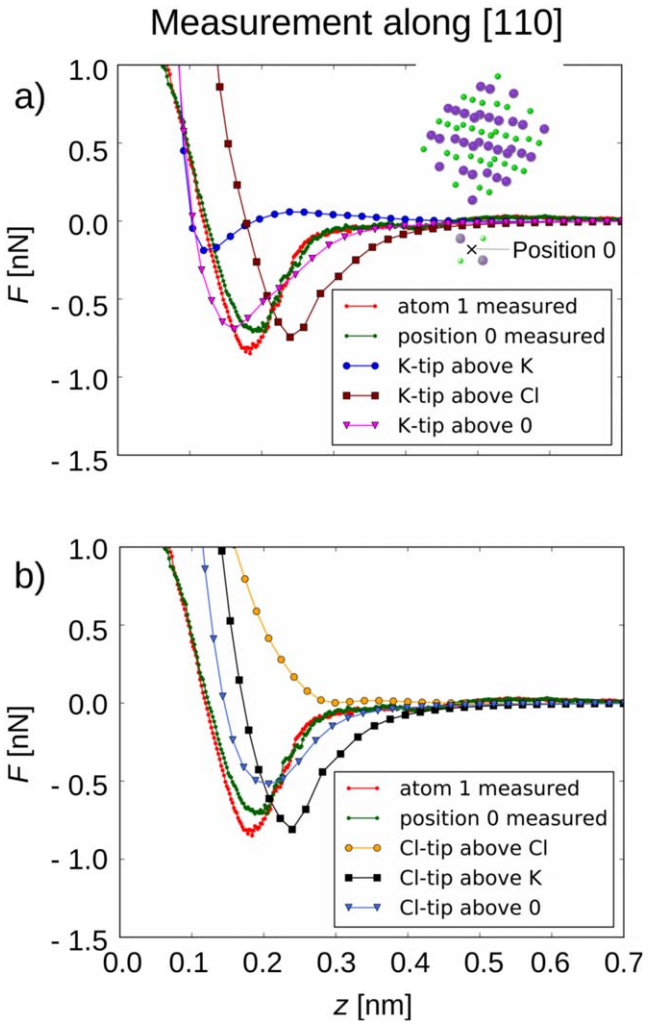

Figure 7. (a) Comparison of force–distance data measured using tip eight along the [110]-direction with the calculated results using a K-terminated tip. (b) Comparison with the calculations using a Cl-terminated tip.

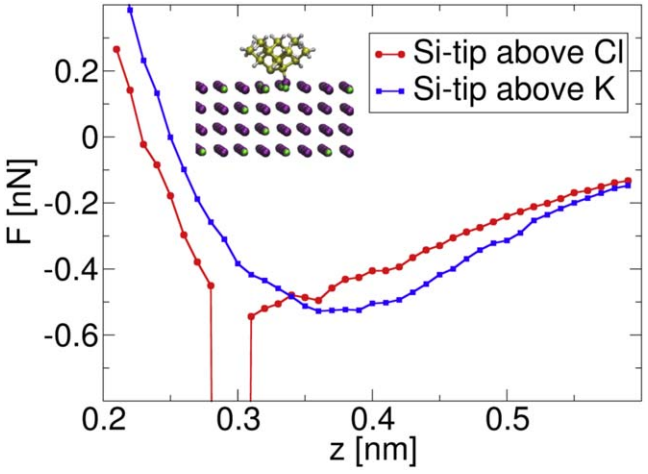

Figure 8. Simulated force for a silicon tip interacting with the KCl surface. Inset shows the atomic configuration during the ionic jump seen at around 0.3 nm above Cl.

positions are different for Cl and K, unlike in experiment. This suggests that the Si-tip is a reasonable model, but we have not captured the exact atomic configuration present in the measurements.

Tilting and/or turning the theoretical tip could improve the overall agreement: the instability occurs when the second atom forming the dimer, i.e. not the atom located at the tip apex but the one slightly behind the tip apex Si atom, attracts a surface atom. If the dimer were tilted in a way that it is more perpendicular to the sample surface plane, the tip-sample distance z where the instability occurs could be pushed to smaller values, to positions closer to the surface and maybe these are not reached in the experiment. This would probably also mean that the z position of the force minimum at this atomic site would be pushed to smaller values—and this would make the difference in the z position of the minimima (between different sites) even larger in the calculations and enhance the difference even more compared to the experimental one. Additionally, turning the tip could move the second atom forming the Si dimer on the tip away from the surface atom it interacts with at the instability. As a result of these considerations, the Si model tip best describes these three tips.

5.3. Two force minima—K-terminated tip

As described above, we defined another group of tips showing two force minima instead of only one. Two tips showed two force minima, tips No. 1 and 5. An example for the force–distance data is shown in figure 9 (tip 5). Both tips show force minima of about 0.3 nN in magnitude. This behavior can be explained well by a movable tip decorated by two additional KCl ions. The two minima are explained by the two different atoms located at the tip interacting with the sample one at larger tip-sample distances and the other at smaller tip-sample distances. Deviations between experiment and calculations could be explained by a different crystallographic orientation of the dimer or by another shape of the tip apex supporting the dimer. Since only the K-terminated tip shows two force minima above both atomic sites as is observed experimentally, it is more likely that the tips used in the experiment were K-terminated.

These movable tips show two force minima for the K-terminated tip with the second minimum being less pronounced for the Cl-terminated tip above Cl and absent for the Cl-terminated tip above K. For a similar tip model for KBr, all four curves had shown two pronounced minima [15].

5.4. Tip with weak tip-sample interaction

One tip could not be grouped in one of the two categories discussed above, tip No. 2. In contrast to the tips of the first category, the maximum attractive force is weaker than 0.5 nN, but the tip shows one single force minimum in contrast to the tips in the second category. A remaining slope of the measured force curve in the distance range between 0.5 to 0.2 nm could indicate that the long-range forces including the elasticity of tip and/or sample might not have been described as

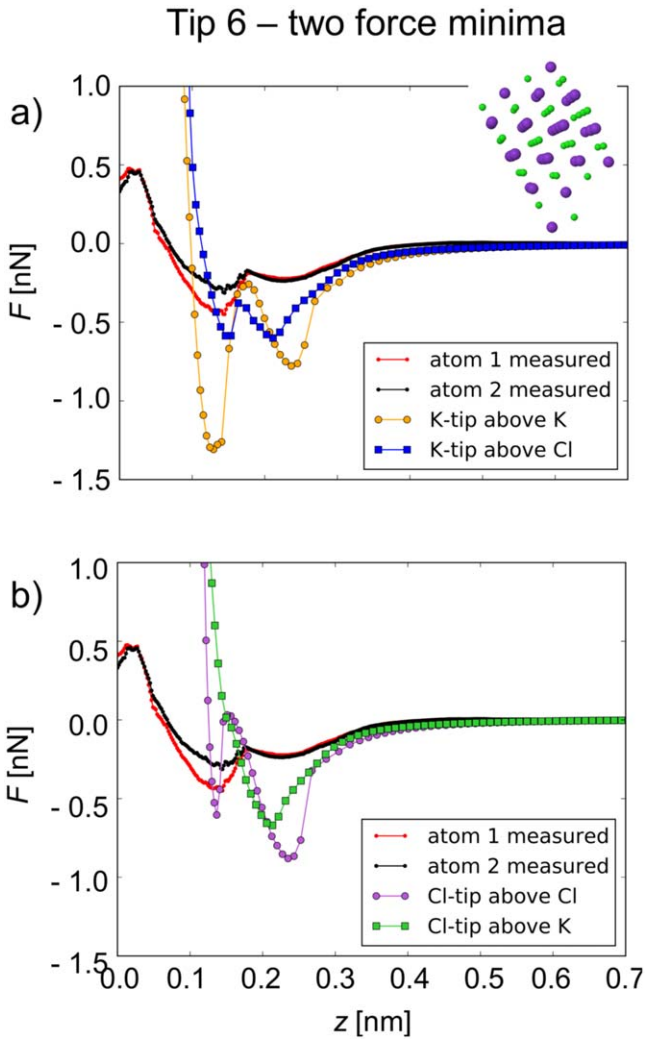

Figure 9. (a) Comparison of force–distance data obtained using tip 5 showing two force minima with the calculated results using a K-terminated tip. (b) Comparison with the calculations using a Cl-terminated tip.

well as for the other tips. If this were the case, and an additional attractive long-range force were subtracted from the data, the force minimum would become even more shallow. This could be a sign for a rather inert tip. In [38] it had been predicted for NaCl that such shallow minima should occur for OH-terminated tips.

5.5. Discussion

In summary, we group the tip mostly into two categories depending on the number of force maxima they show in the force–distance data. One force minimum is expected for an interatomic interaction with no additional atoms, or with a perfectly rigid support of the interacting atoms. A second force minimum can only arise if part of the additional atoms involved in the interaction move significantly out of their equilibrium positions. If the experimental force–distance data shows only one force minimum the tip is more rigid compared to the situation with two force minima. Indeed data obtained from experiments with macroscopic samples show that Si is more rigid than KCl in agreement with our conjecture that the experimental force–distance data showing only one force minimum are best represented by a Si tip.

To compare with an overview on literature results, the KBr-tip used in [7] was K-terminated, the tip used for measurements on KBr in [8] was K-terminated, and the tip used for tuning force measurements in [18] was K-terminated. Even for manipulating Br ions on a NaCl(001) surface doped with Br, the tip remains Na-terminated after vertical manipulation of Br [39]. The tip used on NaCl in [38] was proposed to be a neutral Si-tip. In [40] it was claimed that both tip terminations were found as the tip was switched from one tip termination to the other by crossing a KBr atomic step. Here, as in part of the literature, we also find mainly K-terminated and Si-tips. In view of these results, we could suggest that the tip in [40] might not have been switched from one tip termination to the other, but rather the tip apex atom could have been moved sideways by a suitable fraction of a lattice constant. As a result, there is no clear experimental evidence that halide-terminated tips are observed experimentally, so we tentatively suggest that these tips could be unstable. Our results could be compared to measurements on CaF_2 where both tip terminations were found [4].

The calculations we show here have been performed at zero temperature while the experiments were performed at room temperature. The calculations with the tips with additional K and Cl ion show double minima both for the tip terminations. For the Si-terminated tip there is a strong interaction with the Cl surface ion. These double minima and strong interaction could lead to atomic jumps at room temperature. Here, the energy barriers are too high for thermally activated atomic jumps, e.g. the energy barrier for the jump observed for the Cl-terminated tip in figure 9 is approximately 0.4 eV high, much higher than room temperature. Given the long time window needed for the experiments, on the order of minutes, it is plausible that jumps do occur at room temperature because the small probability for a jump is sampled many times. In addition in previous calculations [15], we have found that for special tip configurations or orientations, smaller energy barriers can occur. These atomic jumps with smaller energy barriers occur in the vicinity of larger jumps, i.e. for example for smaller tip-sample distances or for a slightly different orientation of the tip with respect to the surface. The presence of these double minima could enable tip changes at room temperature necessary to obtain the experimental data used here.

6. Conclusion

We have shown force–distance measurements for a large number of tips, seven tips, on the KCl(001) surface. Atomic resolution is obtained not only in imaging but also in the force–distance data. Tip changes are frequent in these room-temperature measurements leading to experiments performed with atomically different tips. Tip deformations strongly affect force–distance measurements on the KCl(001) surface. For part of the tips used in the experiment, double minima in

the force–distance data are even observed. These double minima arise from atomic-scale tip deformations. In order to explain the complex variations in the force–distance data that depend on the tip, we first find suitable categories such as the number of minima observed and the magnitude of the tip-sample interaction. Then we compare the experimental data to atomistic simulations using KCl tips in different configurations including tips with additional atoms designed for atomic jumps. In addition, we compare the data to first principles simulations with Si tips. The majority of the tips are K- or Si-terminated. While Si-terminated tips show only one force minimum, K-terminated tips show double minima both in experiment and in the calculations.

This relates to the enhanced rigidity of Si compared to KCl. For scanning force microscopy atomic resolution imaging a rigid tip is favorable, because the tip-sample interaction is generally larger and the image contrast formation is simpler. If Si tips are to be used, we recommend to avoid any tip-sample contact for high-resolution imaging of KCl. It could be favorable to use unsputtered Si tips with oxygen-termination for enhanced electrostatic contrast combined with tip rigidity. In addition, we suggest to use a rigid tip coating, e.g. by CaF_2.

Acknowledgments

We thank S Morita for initiating the project and valuable advice, Lev Kantorovich for providing the code used for the atomistic simulations and Thomas Schimmel for stimulating discussions. This work was supported by a Grant-in-Aid for Scientific Research (25106002, 16H00959, 16H00933, 15H03566, 16H03872, 16K13680, 16K13615, 19H05789, 20H05178 and 18H03859) from the Ministry of Education, Culture, Sports, Science and Technology of Japan (MEXT). ASF has been supported by the Academy of Finland through its Centres of Excellence Program Project No. 915 804, and by the World Premier International Research Center Initiative (WPI), MEXT, Japan. ASF acknowledges use of the CSC, Helsinki for computational resources. RHV acknowledges funding from the ERC Starting Grant NANOCONTACTS and from the German Science Foundation through a Heisenberg fellowship.

ORCID iDs

Adam Foster https://orcid.org/0000-0001-5371-5905
Masayuki Abe https://orcid.org/0000-0001-5619-3911
Regina Hoffmann-Vogel https://orcid.org/0000-0003-4984-6210

References

[1] Morita S, Giessibl F J and Wiesendanger R 2009 *Noncontact Atomic Force Microscopy* vol 2 (Berlin: Springer)
[2] Lantz M A, Hug H J, Hoffmann R, van Schendel P J A, Kappenberger P, Martin S, Baratoff A and Güntherodt H-J 2001 *Science* **291** 2580
[3] Custance O, Pérez R and Morita S 2009 *Nat. Nanotechnol.* **4** 803
[4] Foster A S, Barth C, Shluger A L and Reichling M 2001 *Phys. Rev. Lett.* **86** 2373
[5] Sugimoto Y, Pou P, Abe M, Jelinek P, Pérez R, Morita S and Custance O 2007 *Nature* **446** 64
[6] Hoffmann R, Barth C, Foster A S, Shluger A L, Hug H J, Güntherodt H-J, Nieminen R M and Reichling M 2005 *J. Am. Chem. Soc.* **127** 17863
[7] Hoffmann R, Kantorovich L N, Baratoff A, Hug H J and Güntherodt H-J 2004 *Phys. Rev. Lett.* **92** 146103
[8] Ruschmeier K, Schirmeisen A and Hoffmann R 2008 *Phys. Rev. Lett.* **101** 156102
[9] Mohn F, Gross L, Moll N and Meyer G 2012 *Nat. Nano* **7** 227–31
[10] Ooe H, Kirpal D, Wastl D S, Weymouth A J, Arai T and Giessibl F J 2016 *Appl. Phys. Lett.* **109** 141603
[11] Langlais V, Guillermet O, Martrou D, Gourdon A and Gauthier S 2016 *J. Phys. Chem.* C **120** 18151
[12] Neff J L, Milde P, Pérez León C, Kundrat M D, Eng L M, Jacob C R and Hoffmann-Vogel R 2014 *ACS Nano* **8** 3294
[13] Schulzendorf M, Hinaut A, Kisiel M, Jöhr R, Pawlak R, Restuccia P, Meyer E, Righi M C and Glatzel T 2019 *ACS Nano* **13** 5485
[14] Hoffmann R, Baratoff A, Hug H J, Hidber H R, v Löhneysen H and Güntherodt H-J 2007 *Nanotechnology* **18** 395503
[15] Ittermann B, Hoffmann-Vogel R, Behrens L and Baratoff A 2013 *Phys. Rev.* B **87** 195437
[16] Lantz M A, Hoffmann R, Foster A S, Baratoff A, Hug H J, Hidber H R and Güntherodt H-J 2006 *Phys. Rev.* B **74** 245426
[17] Kawai S, Canova F F, Glatzel T, Foster A S and Meyer E 2011 *Phys. Rev.* B **84** 115415
[18] Such B, Glatzel T, Kawai S, Koch S and Meyer E 2010 *J. Vac. Sci. Technol.* B **28** C4B1
[19] Yokoyama K, Ochi T, Uchihashi T, Ashino M, Sugawara Y, Suehira N and Morita S 2000 *Rev. Sci. Instrum.* **71** 128
[20] Albrecht T R, Grütter P, Horne D and Rugar D 1991 *J. Appl. Phys.* **69** 668
[21] Sugimoto Y, Namikawa T, Miki K, Abe M and Morita S 2008 *Phys. Rev.* B **77** 195424
[22] Yi I, Nishi R, Abe M, Sugimoto Y and Morita S 2011 *Japan. J. Appl. Phys.* **50** 015201
[23] Sirdeshmukh D, Sirdeshmukh L and Subhadra K 2013 *Alkali Halides: A Handbook of Physical Properties* (Berlin: Springer)
[24] Sader J E and Jarvis S P 2004 *Appl. Phys. Lett.* **84** 1801
[25] Sader J E, Hughes B D, Huber F and Giessibl F J 2018 *Nat. Nanotechnol.* **13** 1088
[26] Fremy S, Kawai S, Pawlak R, Glatzel T, Baratoff A and Meyer E 2012 *Nanotechnology* **23** 055401
[27] Sangster M J L and Atwood R M 1978 *J. Phys. C: Solid State Phys.* **11** 1541
[28] Kresse G and Furthmüller J 1996 *Comput. Mater. Sci.* **6** 15
[29] Kresse G and Furthmüller J 1996 *Phys. Rev.* B **54** 11169
[30] Klimeš J, Bowler D R and Michaelides A 2010 *J. Phys.: Condens. Matter* **22** 022201
[31] Klimeš J, Bowler D R and Michaelides A 2011 *Phys. Rev.* B **83** 195131
[32] Björkman T, Gulans A, Krasheninnikov A V and Nieminen R M 2012 *Phys. Rev. Lett.* **108** 235502
[33] Blöchl P E 1994 *Phys. Rev.* B **50** 17953
[34] Martsinovich N and Kantorovich L 2008 *Phys. Rev.* B **77** 115429
[35] Argento C and French R 1996 *J. Appl. Phys.* **80** 6081

[36] Guggisberg M, Bammerlin M, Loppacher C, Pfeiffer O, Abdurixit A, Barwich V, Bennewitz R, Baratoff A, Meyer E and Güntherodt H-J 2000 *Phys. Rev.* B **61** 11151
[37] Bergström L 1997 *Adv. Colloid Interface Sci.* **70** 125
[38] Hoffmann R, Weiner D, Schirmeisen A and Foster A S 2009 *Phys. Rev.* B **80** 115426
[39] Kawai S, Foster A S, Canova F F, Onodera H, Kitamura S-I and Meyer E 2014 *Nat. Commun.* **5** 4403
[40] Venegas de la Cerda M A, Abad J, Madgavkar A, Martrou D and Gauthier S 2008 *Nanotechnology* **19** 045503